Identification of a Seeding Signature in Texas Using Multi-Spectral Satellite Imagery

By

William L. Woodley, President
Woodley Weather Consultants
Littleton, Colorado

Daniel Rosenfeld, Professor
Hebrew University of Jerusalem
Jerusalem, Israel

Aldis Strautins,
Project Manager
West Texas Weather Modification Association
San Angelo, Texas

Abstract. The method of Rosenfeld and Lensky (1998a) to infer cloud microstructure using multi-spectral, AVHRR, satellite imagery is being used in Texas to determine whether operational cloud seeding is producing recognizable changes in cloud microstructure. The seeding signature is expected to take the form of ice formation at relatively warm temperatures (i.e., > -10°C) as is required by the conceptual model guiding the seeding programs (Rosenfeld and Woodley, 1993).

Two cases are presented. The first on 10 August 1999 involved seeding with ejectable silver iodide flares near cloud top and the second on 28 August 1999 involved seeding in updraft regions near cloud base with silver iodide generators and flares affixed to the wings of the seeder aircraft. Both apparently produced seeding signatures. The analysis of the first case suggests anomalous glaciation was achieved in the seeded clouds at –13°C whereas it was achieved at about –19°C to –21°C in the clouds in other areas. These differences are consistent with an effect of seeding in that the seeded clouds glaciated at a warmer temperature than the other clouds.

The second case involved operational seeding in the target area of the West Texas Weather Modification Association. Base silver iodide seeding of a short cumulonimbus line began 56 min before the pass of the monitoring satellite when the line was in its formative stages. The maximum updraft at cloud base was estimated at 3,000 ft/min along the line just before the satellite overpass. The analysis revealed a strong apparent seeding signature in the cloud line. The signature took the form of complete glaciation at about –9°C, whereas other similar clouds in the region glaciated between –20°C to –30°C. This appears to constitute a strong glaciation signature resulting from the seeding at cloud base.

The detection of apparent seeding signatures in Texas is an important development. It indicates that the top and base AgI seedings are producing ice at temperatures around –10°C. According to the conceptual model guiding the operational seeding programs in Texas, this should be the first step in the process leading to more rainfall. The TEXARC research program has already established that the seeding agents used in Texas produce more ice in individual clouds, but such glaciation had never been documented on a scale that can be seen by satellite sensors until this study. There is now greater reason to take the next step and look for increases in rainfall as a result of the seeding.

1. INTRODUCTION

The method of Rosenfeld and Lensky (1998a) to infer cloud microstructure using NOAA-14, multi-spectral, AVHRR, satellite imagery was used in Texas in 1999 for four purposes. First, the method was used to look for evidence that pollution is affecting the rain-forming processes in Texas clouds. Second, it was used to determine whether operational cloud seeding produces recognizable changes in cloud microstructure that are consistent with conceptual, cold-cloud, seeding models. Third, the technique was used to demonstrate its potential for assessing in real time when and where seeding should be conducted and what type of seeding should be employed. Fourth, the method was used to classify the cloud microstructure prevalent on each day of the summer within each of the seven operational targets. This information will be used for partitioning the days during the analysis phase of the operational cloud seeding experiments. Woodley and Rosenfeld (1999) provide the results of this research effort. Bomar et al. (1999) provides background information on the Texas operational seeding programs.

This paper deals with the second purpose, the detection of a seeding signature in the cloud seeding programs of Texas (see Bomar et al., 1999). The seeding signature is expected to take the form of ice formation at relatively warm temperatures (i.e., ≥ -10°C) as is required by the conceptual model guiding the seeding programs (Rosenfeld and Woodley, 1993).

2. INFERRING CLOUD MICRO-STRUCTURE WITH SATELLITES

The method to infer cloud microstructure from space is addressed by (1998a). It makes use of data from the Advanced Very High Resolution Radiometer (AVHRR) onboard the NOAA operational weather satellites, which provide sub-satellite 1.1 km data in 5 channels centered at 0.65, 0.9, 3.7. 10.8, and 12.0 microns. The visible wave band (0.65 microns) is used to select points with visibly bright clouds for the analyses. The thermal infrared (10.8 and 12.0 microns) is used to obtain cloud-top temperatures. Cloud-top particle size is inferred from the solar radiation component of the 3.7-micron wave band. The method works also with the VIRS sensors on the TRMM (Tropical Rainfall Measuring Mission) satellite.

In making the inferences of cloud microphysical structure, the effective radius (r_{eff}) of fully cloudy pixels is retrieved in the manner described by (1998a). This is done by inverting a radiative transfer model developed by Nakajima and King (1990), using the solar reflectance component of the 3.7 micron channel and the viewing geometry as inputs. Retrieval of particle size at cloud top is based on the fact that water absorbs part of the solar radiation at the 3.7micron wave band. While the back-scattered solar radiation is determined mainly by the surface area of the particles, the amount of absorption is determined by the volume of the particles. Therefore, larger particles absorb more and reflect less, so clouds that are made of larger droplets are seen darker in the reflected 3.7micron radiation.

Knowing the energy radiated from the sun and the portion of that energy reflected back to the satellite sensor, the fraction of the solar energy absorbed can be retrieved. This provides the basis for calculating the ratio between the integral volume and integral surface area of cloud particles in the satellite measurement volume. Conventionally, this ratio has been defined as the particle effective radius, r_{eff}.

The initial research suggests that a r_{eff} of 14 microns is a threshold value above which clouds contain precipitation-size particles that can be detected by weather radar (Rosenfeld and Gutman, 1994; Lesnsky and Rosenfeld, 1997). The maximum value of r_{eff} that can be retrieved by this method is 34 microns.

The evolution of r_{eff} as a function of cloud-top height or temperature (T) of growing convective elements can reveal the microphysical evolution of the clouds as they grow vertically and undergo the various microphysical process that lead to the formation of precipitation. However, the satellites carrying high-resolution AVHRR sensors typically provide only a twice-daily snapshot image of a specific portion of the earth. Thus, a single cloud cannot be viewed continuously in the imagery. This difficulty is overcome by observing an area containing a convective cloud cluster composed of cloud elements at various stages of vertical growth. This allows the compositing of the r_{eff} calculations for many clouds as if they represented a singe cloud at different times in its lifetime.

The actual composite is done in the following steps:

a) Define a window, typically of several thousand pixels, encompassing convective cloud clusters with growing elements at various stages of development.
b) Calculate the median and other percentiles of the r_{eff} for pixels within each 1°C interval of cloud top temperature (T).
c) Display graphically the T vs. r_{eff} curves of various percentiles, so that both the dependence and spread of r_{eff} as a function of T can be shown.
d) Analyze the shape of a specific T-r_{eff} curve (e.g., the median, which is the 50th percentile) to find the microphysical zones as discussed below.

The shape of the T vs. r_{eff} diagrams contains much information on the microphysical processes in the clouds. It is known that droplets grow by diffusion a small distance above the base of convective clouds while higher up in the clouds the hydrometeor growth rate is often accelerated by coalescence and ice processes. Because nearly all cloud droplets are nucleated at cloud base and cloud water mass increases less than linearly with depth, it is found that the r_{eff} in clouds with mostly diffusional growth increases by a power law of less than $D^{1/3}$, where D is depth above cloud base. D can be approximated using T_b-T, where T and T_b are cloud top and base temperatures, respectively.

It can then be seen that r_{eff} is proportional to $(T_b\text{-}T)^{1/3}$ and a plot of r_{eff} versus temperature will look like an upward convexed curve. Therefore, a deviation from such a curve (i.e., an upward concave curve) indicates the existence of amplification mechanisms for the cloud-particle growth rate, such as coalescence and ice formation processes, which lead ultimately to precipitation.

The evolution of convective cloud-top particles as a function of depth above cloud base and cloud-top temperature can be characterized into five distinct vertical zones, not all necessarily appearing in a given cloud system:

1) *Diffusional droplet growth zone:* Very slow growth of cloud droplets with depth above cloud base, indicated by shallow slope of dr_{eff}/dT.

2) *Droplet coalescence growth zone:* Large increase of the droplet growth rate dr_{eff}/dT at $T > 0°C$, indicating rapid growth of the cloud droplets with depth above cloud base. This can only occur by drop coalescence.

3) *Rainout zone:* A zone where r_{eff} remains stable at about 20 microns, probably determined by the maximum drop size that can be sustained by rising air near the cloud top, where the larger drops are precipitated to lower elevations and may eventually fall as rain from the cloud base. This zone is so named, because the clouds seem to be raining out much of their water while growing. The radius of the drops that actually rain out from cloud tops is much larger than the indicated r_{eff} of 20 microns, being at the upper end of the drop size distribution.

4) *Mixed phase zone:* A zone in which ice first appears along with the existing liquid water. The onset of the mixed-phase zone is a function of the regimes in which the cloud hydrometeors are growing as they rise to temperatures < 0°C. If the droplets are growing by diffusion, the onset of ice is set to the temperature at which the particle size begins to increase rapidly, indicating the growth of ice particles. This is normally about –10°C. If, however, the droplets are already growing by coalescence as they enter the supercooled zone, the onset of the mixed-phase zone is set to –6°C. This is based on observations from cloud physics aircraft. In the extreme, if the drops are already raining out at temperatures ≥ 0°C, the onset of the mixed-phase zone begins at the top of the rainout zone. Such behavior is characteristic of highly maritime clouds with early rainout and glaciation, often at temperatures ≥ -5°C (Rosenfeld and Lensky, 1998b).

5) *Glaciated zone:* A nearly stable r_{eff} zone at below freezing temperatures at a value greater than that of the rainout zone. The value is probably determined by the maximum ice particle size that can be sustained near cloud top, where the larger particles are precipitated to lower elevations while aggregating and forming snowflakes. The onset of the glaciation zone occurs when the 30th percentile plot of the r_{eff} first reaches 30 microns in the mixed-phase zone.

Examples of the above cloud-microphysical zones as inferred from the AVHRR imagery in Texas are provided in Figures 1 to 3. Each zone was determined objectively using algorithms that codify the definitions above. Plotted are the 5th through the 100th percentiles (inclusive), every 5%, of the r_{eff} for each 1°C interval. The median (50th percentile) is indicated by the interface between the yellow and green lines. The 30th percentile (interface between green and blue) was used for the classification of microphysical zones in this study. The number of data points as a function of temperature (height) is indicated by the white line.

To facilitate visualization of the information in Figures 1 to 3 in the three spectral channels and the physical processes operative in the clouds, the satellite images are color-coded. In the visible channel very bright clouds are red while clouds dim to the eye have little red. The 3.7-micron channel is used to infer drop size, where clouds with very small drops are green and those with large drops have no green. The 10.8-micron channel is used to infer cloud top temperature. Warm surfaces are blue while very cold surfaces have no blue.

Upon combining the information in the three channels, the three basic colors (red, blue and green) are combined to produce a colorized image along with the plots of effective radius vs. temperature. Thus, supercooled clouds will appear yellow in the images, which is the resultant of some green (small drops) and some red (bright clouds) but little blue (supercooled cloud tops). Conversely, clouds with coalescence at low levels will appear magenta, which is the combination of some red (bright clouds) and some blue (relatively warm cloud tops) but little green, because the drops are large. A full description of the color codes and color pallets was published by Rosenfeld and Lensky (1998a).

The first image illustrates highly continental clouds with deep zones of diffusional growth and virtually no coalescence. The image at 2212 GMT on 30 May 1999 shows a field of clouds in west Texas between Midland and Del Rio that include cumulonimbus clouds having a yellow-orange tint (Figure 1). This coloration suggests the clouds are bright but contain small particles. The plots of effective radius (r_{eff}) vs. temperature on the left side of the figure show this is true. Note the clouds in both Areas 1 and 2 have a deep zone of diffusional growth (vertical yellow line) with only a slow increase of r_{eff} with a decrease in temperature. The effective radius does not reach the 14-micron threshold for precipitation formation until the clouds are well supercooled. Such clouds are highly inefficient precipitators.

The clouds in Areas 1 and 2 have a mixed-phase zone (vertical purple line), which exists above the zone of diffusional growth. It begins at about –20°C, where the r_{eff} growth rate increases due to the formation and growth of ice particles.

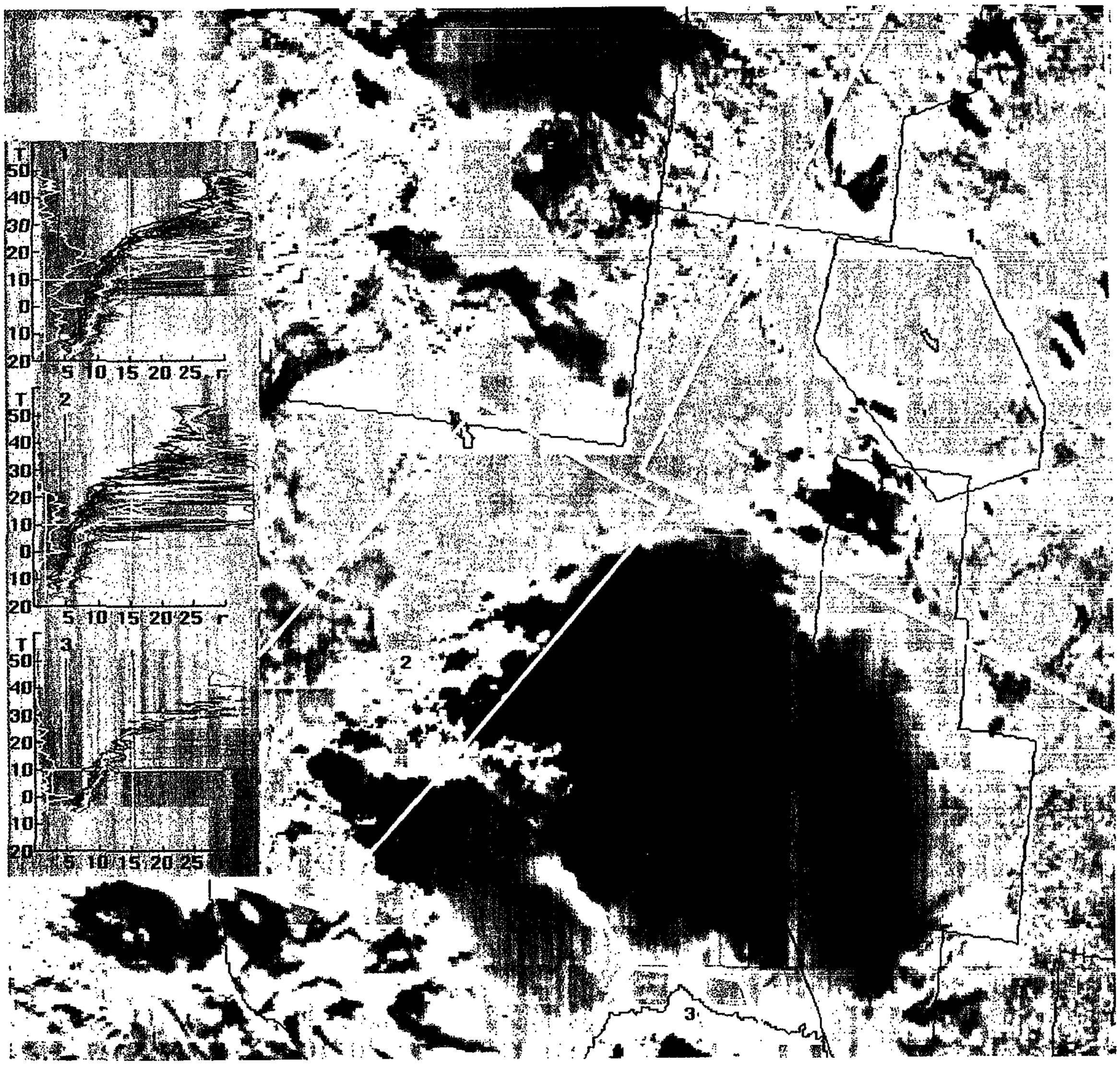

Figure 1. Processed NOAA-14 satellite image at 2212 GMT (1646 CDT) on 30 May 1999. See text for details.

The clouds of Areas 1 and 2 do not glaciate until about –34°C and –40°C, respectively, where a glaciated cloud is defined as one in which practically all of its water has turned into ice particles. Cloud-top glaciation occurs usually at temperatures of –5°C to -10°C for clouds with well-developed coalescence, typical of maritime clouds in agreement with the laboratory experiments of Hallett and Mossop (1974). Glaciation occurs typically at about –15°C for continental clouds with some coalescence or at –20°C for more continental clouds. In the extreme, glaciation can occur at temperatures as cold as –38°C for highly continental clouds (Rosenfeld and Woodley, 2000). It can be seen, therefore, that the clouds in the image on 30 May 1999, including those in Area 3 in Mexico, were extremely continental.

At the other extreme are clouds with little diffusional growth, rampant coalescence and early glaciation. An example is provided in Figure 2 for 21 June 1999 at 2125 GMT. Big Spring and Lubbock, Texas are at the bottom center and left center of the image, respectively. Most of the clouds in Area 2 are distinctly purple and magenta. The r_{eff} plot vs. temperature shows a shallow zone of coalescence growth (vertical green line) overlain by a zone of warm precipitation fallout (vertical blue line), a shallow mixed-phase zone beginning near 0°C (vertical magenta line) and finally a deep zone of glaciation (vertical red line). The rainout zone can exist only in clouds with well-developed coalescence that has progressed to the extent that further increase of drop size is compensated by the fallout of large drops from the cloud tops. Therefore, the rainout zone exists just above the droplet coalescence growth zone in highly maritime clouds. Such clouds are probably not suitable for any kind of seeding intervention.

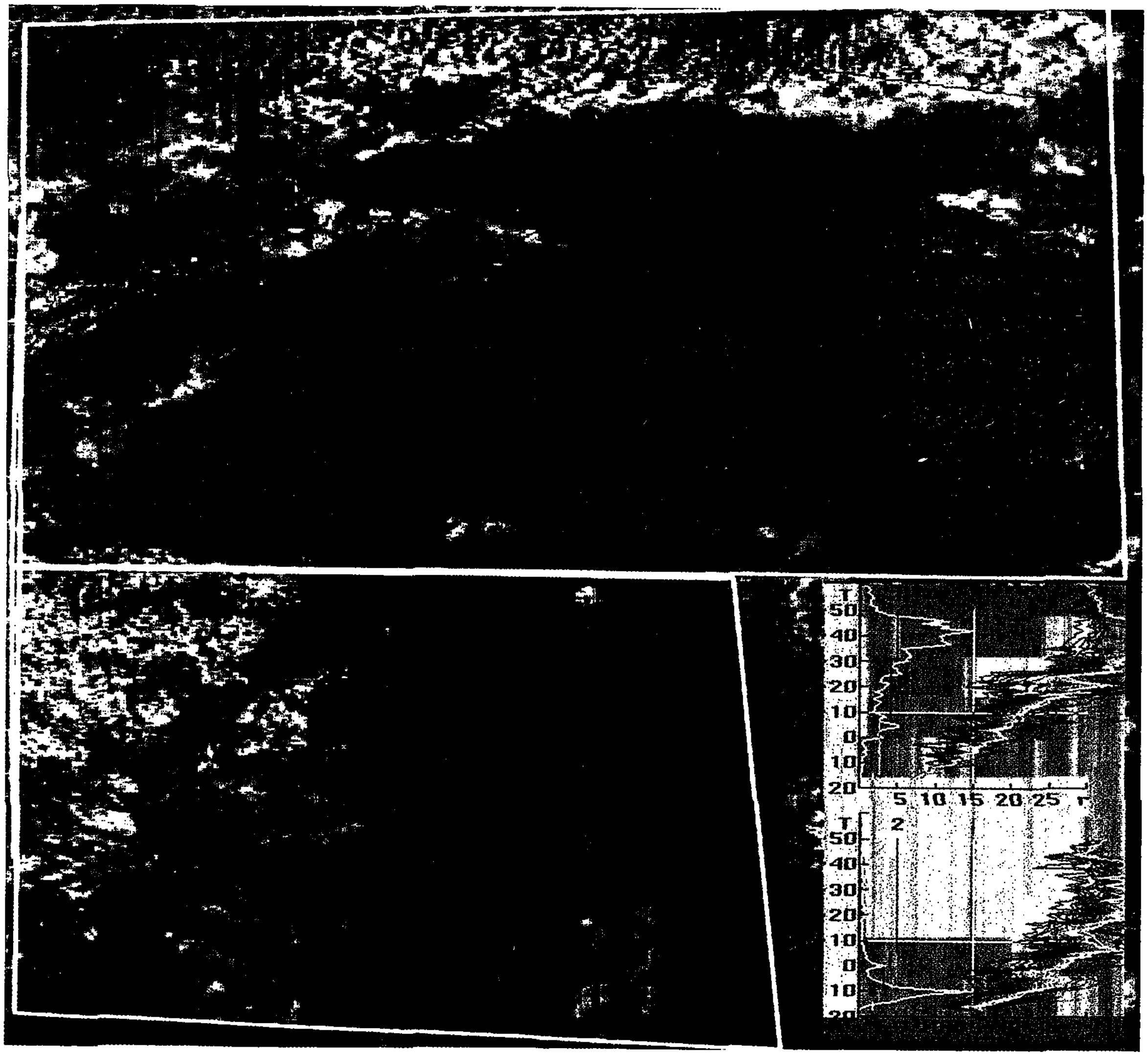

Figure 2. Processed NOAA-14 satellite image at 2125 GMT (1625 CDT) on 21 June 1999. See text for details.

In contrast to Area 2, however, are the clouds and r_{eff} plots for Area 1 to the north of Area 2. Here too coalescence starts at low levels, but the mixed-phase zone is much deeper and onsets at a colder temperature. Complete glaciation is not indicated until about −30°C. This suggests that the clouds of Area 1 were much more vigorous and had stronger updrafts than those of Area 2, such that their hydrometeors were carried to much greater heights before freezing was complete. That is consistent with the lack of a rainout zone in Area 1, because there is no time for rainout in strong updrafts. These clouds might even have developed small hail within their deep mixed-phase zones before glaciation was complete. Only with this processed satellite imagery could such intriguing spatial variability in cloud characteristics have been discerned on this day.

An example of clouds midway between the extremes of Figures 1 and 2 is provided in Figure 3 for 3 August 1999 at 2146 GMT. The cloud cluster of interest is north and northeast of Del Rio. The plots of r_{eff} vs. temperature suggest little to no diffusional droplet growth (vertical yellow line) and rather deep zones of coalescence growth (vertical green line). The clouds in Areas 2 and 3 reach the 15-micron threshold for precipitation formation at a temperature of about +5°C while it is about 0°C in Area 1. The mixed-phase (magenta vertical line) and glaciation zones (the vertical red line) begin at warmer temperatures than on 30 May 1999, when there was much less coalescence activity. Even so, full glaciation does not take place on 3 August 1999 until temperatures $\leq$ -25°C in all areas. This is likely due to rather strong updrafts, which carry the liquid hydrometeors to rather cold temperatures before they have the chance to freeze.

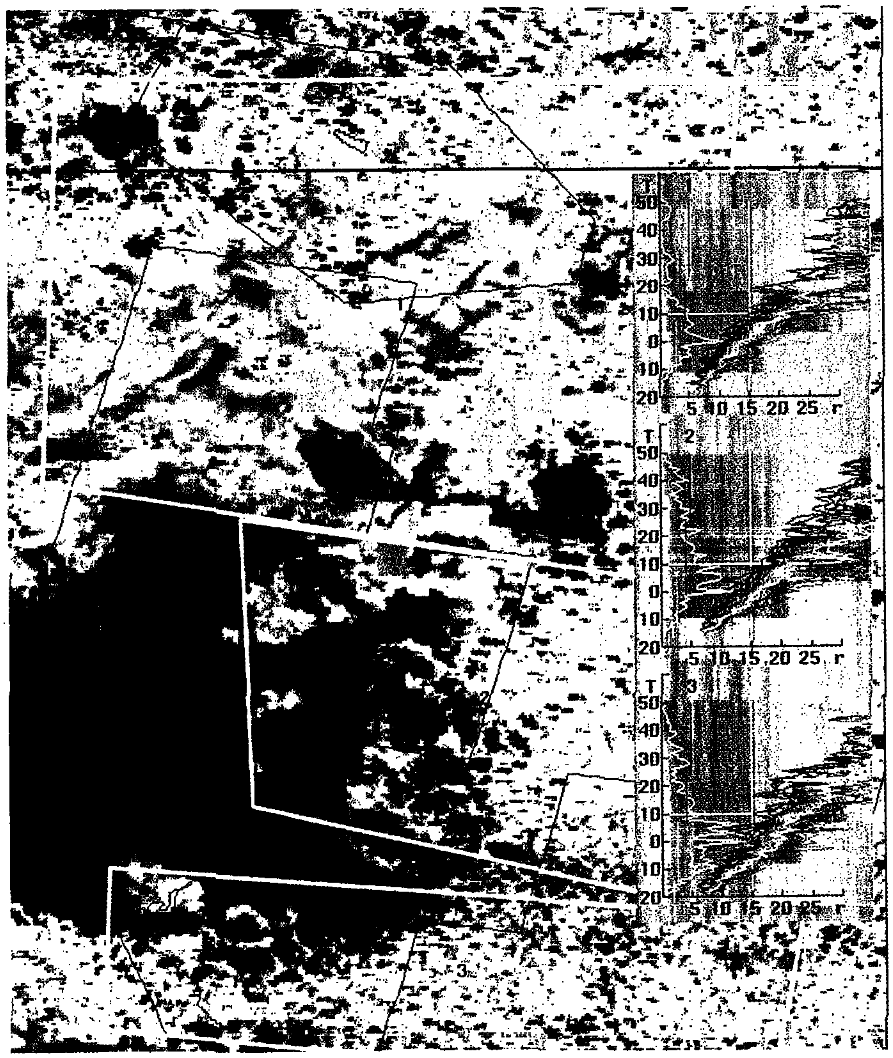

Figure 3. Processed NOAA-14 satellite image at 2146 GMT (1646 CDT) on 3 August 1999. See text for details.

From all appearances the clouds of 3 August 1999 should have been highly suitable for AgI seeding intervention, according to the conceptual seeding model articulated by Rosenfeld and Woodley (1993). The clouds had strong updrafts filled with supercooled rain in which AgI nuclei could act to freeze the raindrops to form graupel particles, which could then grow rapidly in the invigorated updrafts. According to the conceptual model, this should lead ultimately to increased rainfall.

3. SEEDING SIGNATURES

It is clear from the previous section that the Rosenfeld methodology can be used to infer the microstructure of convective clouds. Having established this, the next question was whether it could be used to document changes in cloud microstructure due to cloud seeding, especially enhanced glaciation at temperatures $\geq$ -10°C. Several cases have been analyzed so far and most suggest seeding acted to increase ice in the clouds as intended, as a precursor to the enhancement of the rainfall

"REVIEWED"

(Woodley and Rosenfeld, 1999). Two of the more interesting cases are presented here. The first on 10 August 1999 involved seeding with ejectable silver iodide flares near cloud top and the second on 28 August 1999 involved seeding in updraft regions near cloud base with silver iodide generators and flares affixed to the wings of the seeder aircraft. Each case was analyzed using the Rosenfeld methodology.

On 10 August 1999 groups of suitable convective clouds were seeded from the Lear jet of Weather Modification, Inc. with ejectable AgI flares within 30 min of the overpass of the NOAA-14 satellite. The processed image at 1707 CDT on 10 August 1999 (Figure 4) shows a N-S region of convection in eastern New Mexico. The three areas in the image correspond to the three plots of r_{eff} vs. temperature. Silver iodide seeding was done in two clouds in area 1 with the expenditure of 10 flares in the half-hour prior to the satellite overpass. Areas 2 and 3 were selected because they contain clouds comparable in size to those in Area 1. Photographs of the clouds just before and 10-min after they were seeded are provided in Figure 5. The cloud outline appeared hard prior to treatment, indicating mostly supercooled cloud water, and soft and frizzy afterwards, indicating the seeding-induced conversion of the water to ice. Plots (not shown) of the passes of the cloud physics aircraft verified the rapid conversion to ice.

The satellite analysis also indicates the clouds were glaciated. The objective glaciation algorithm indicates glaciation was achieved (bottom of vertical red line) in Area 1 at −13°C whereas it is achieved at

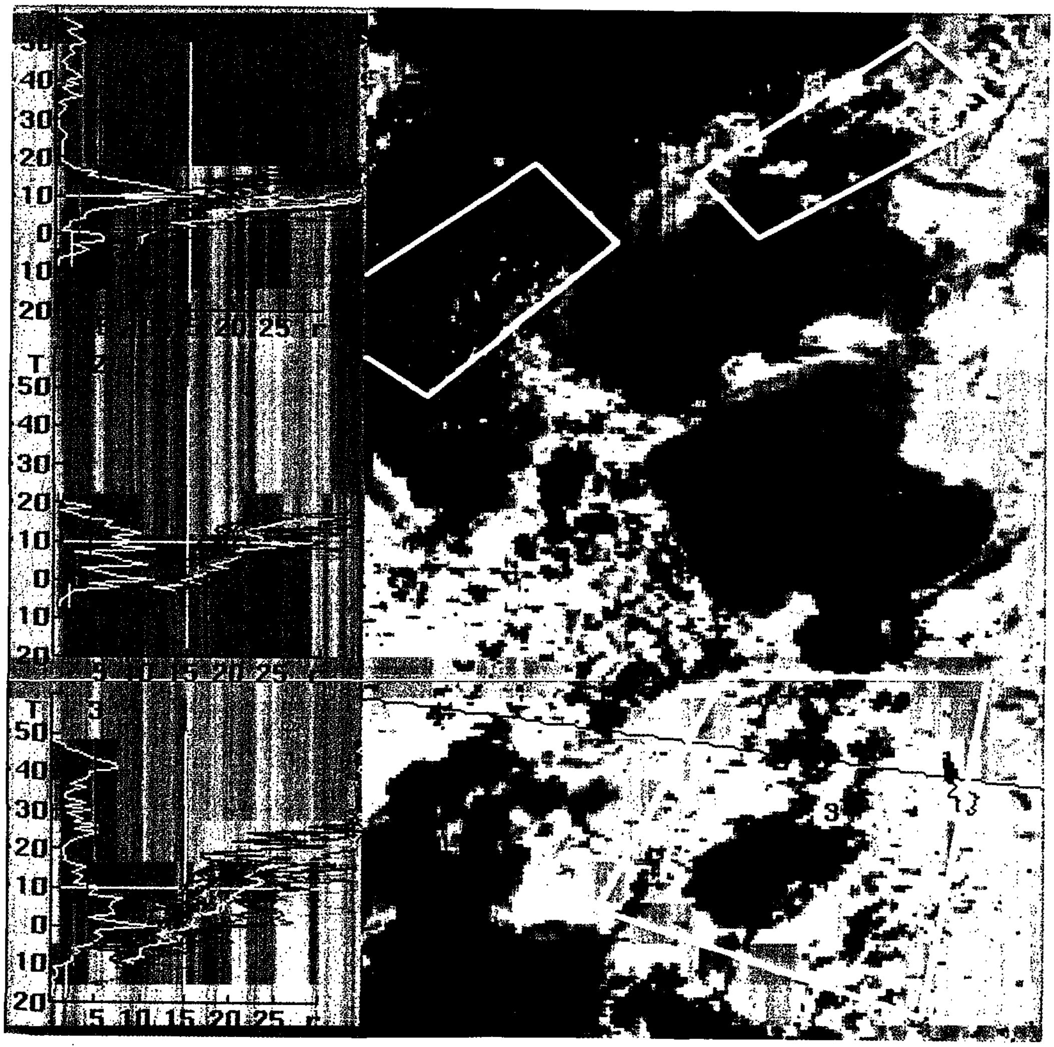

Figure 4. Colorized satellite image produced using the methodology of Rosenfeld and Lensky (1998a) from the NOAA-14 overpass of Texas at 2207 GMT (1707 CDT) on 10 August 1999. Plots of effective radius (r_{eff}) vs. temperature for the clouds in the three marked areas in the image appear as insets on the left side of the figure. An explanation is provided in the text.

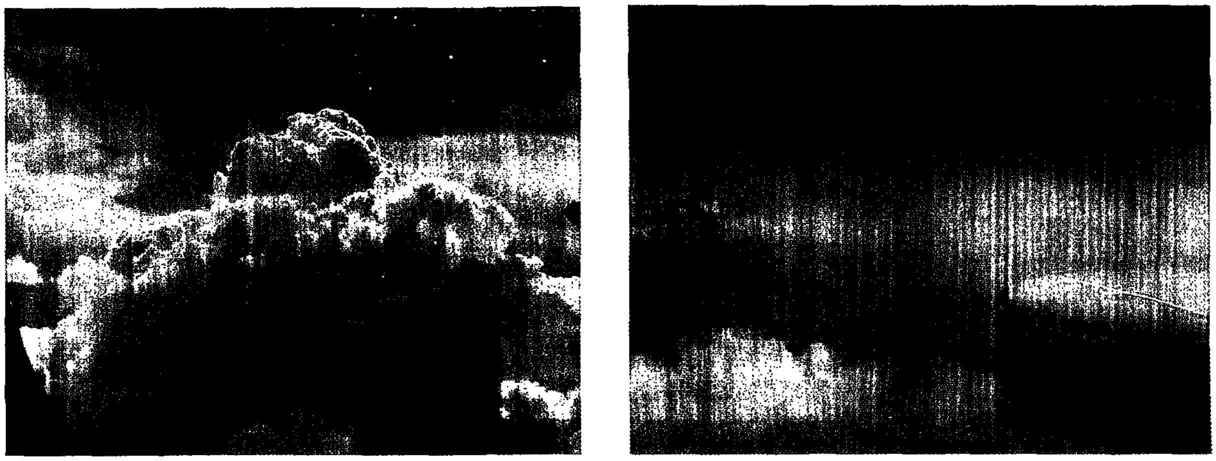

Figure 5. Hand-held photographs taken by Dr. Rosenfeld from the Lear jet cloud physics aircraft on 10 August 1999. The first photograph was taken as the aircraft approached the cloud. The second was taken 10-min later after the cloud had been seeded and turned to ice.

–19°C and –21°C in areas 2 and 3, respectively. These differences are consistent with an effect of seeding in that the clouds in Area 1 glaciated at a warmer temperature than in Areas 2 and 3. Note that all plots indicate the clouds contained coalescence and precipitation-sized particles, beginning at temperatures < 0°C.

A second intriguing case involved an instance of operational seeding in the target area of the West Texas Weather Modification Association (WTWMA) on 28 August 1999. The color-coded satellite imagery for this case for the NOAA-14 pass beginning at 2203 GMT (1703 CDT) is shown in Figure 6. San Angelo, Texas is at the center of the image. Maps of portions of four of the seven targets of the seeding programs operative in Texas in 1999 are superimposed on the image. The eastern two-thirds of the WTWMA target can be seen in the left center of the image. The three additional irregular areas with light red boundaries numbered 1, 2 and 3 in Figure 6 enclose the clouds that were subjected to analysis.

Looking first at the colorized clouds, there are several masses of cumulonimbus clouds appearing bright red to signify bright (very red) and cold (no blue) clouds with large ice particles (no green). Most of the smaller cumuli and feeders to the cumulonimbus clouds are yellow to light pink to signify towering cumuli (a little blue) of moderate brightness (some red) with small particles (some green). The resultant is yellow, which indicates the clouds contain supercooled cloud water. The large cloud masses were propagating to the southwest as they grew on their south and west sides and dissipated on their north flanks.

The cloud mass of primary interest in the satellite image is the short, colorized, cumulonimbus line oriented NW-SE in and outside the target area of the West Texas Weather Modification Association (Area 1 in Figure 6). Seeding of this cloud mass in its formative stages had begun just inside the target on the northwest edge of the line at 1607 CDT, 56 min before the satellite overpass at 1703 CDT. Seeding was done continuously using a silver iodide (AgI) generator with an output of 2.8 gm/min. In addition, 40-gm "burn-in place" AgI flares were ignited when the updraft exceeded 1,000 ft/min. Seven such flares were ignited prior to the satellite overpass, bringing the total expenditure of AgI to 437 gm prior to the satellite overpass. Both flares and burner produced condensation-freezing nuclei with 90% of the nuclei activated within 5 minutes of their generation. Based on laboratory tests, it is estimated that this amounted to the production of at least 10^{15} ice nuclei active at –10°C, assuming coagulation effects are negligible (an arguable assumption). Seeding progressed up and back along the southern edge of the line with time. The maximum updraft at cloud base was estimated at 3,000 ft/min along the line just before the satellite overpass. These are ideal conditions for base seeding, and it is quite likely that the nucleant reached the tops of the vigorous clouds as intended.

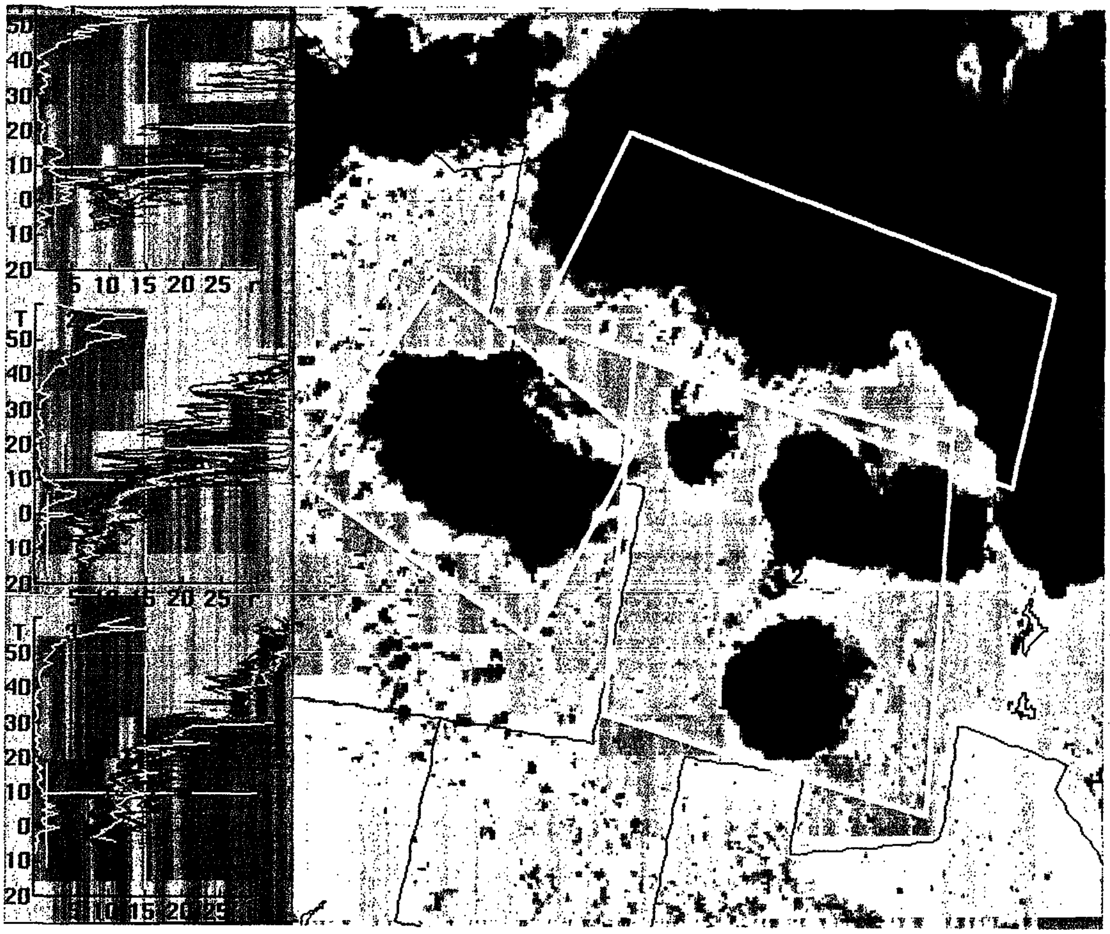

Figure 6. Colorized satellite image produced using the methodology of Rosenfeld (Rosenfeld and Lensky 1998a) from the NOAA-14 overpass of Texas at 2203 GMT (1703 CDT) on 28 August 1999. Plots of effective radius (r_{eff}) vs. temperature for the clouds in the three marked areas in the image appear as insets on the left side of the figure. An explanation is provided in the text.

Documentation of the seeding along the aircraft track and the development of the line on radar through 1724 CDT is provided in Figures 7a-7d from the output of the TITAN system that has been installed on the WTWMA radar. The white line in each panel is the track of the aircraft. One silver iodide acetone burner was on continuously along this track. The identifiers F1 through F9 indicate the locations where burn-in-place (BIP) AgI flares were ignited. Although the identifiers appear in each plot, the flares are not ignited until the aircraft track passes through the identifier. A total of 18 flares, 11 after the satellite overpass, were ignited below cloud base in this line along with the continuous burn of the AgI generator. A complete history of the event is given in Table 1.

The numbers in yellow superimposed on the radar images give the tops of the radar echoes in kilometers at the time of the radar scan that appears under each of six panels in each figure. The intensity of the color-contoured echoes can be determined by matching the colors with the scale that appears on the right of each figure. An echo having a yellow core has an intensity exceeding 51 dBZ but not more than 54 dBZ.

Examination of Figures 7a to 7d revealed the following:

- The echo mass has the same shape as the cloud mass in the satellite image (see Figure 6).
- The seeding covered the entire length of the line but the return time to a particular spot along the line was on the order of 20 minutes.
- The rain was heavy at several places along the line as it propagated to the southwest.
- The maximum echo top height was 15.5 km (51,000 ft) at 16:32:45 CDT along the border of the WTWMA target.
- It was raining at several points along the line when seeding commenced.
- Each BIP flare was ignited at the leading edge of the line on radar.

August 28, 1999

Figure 7a

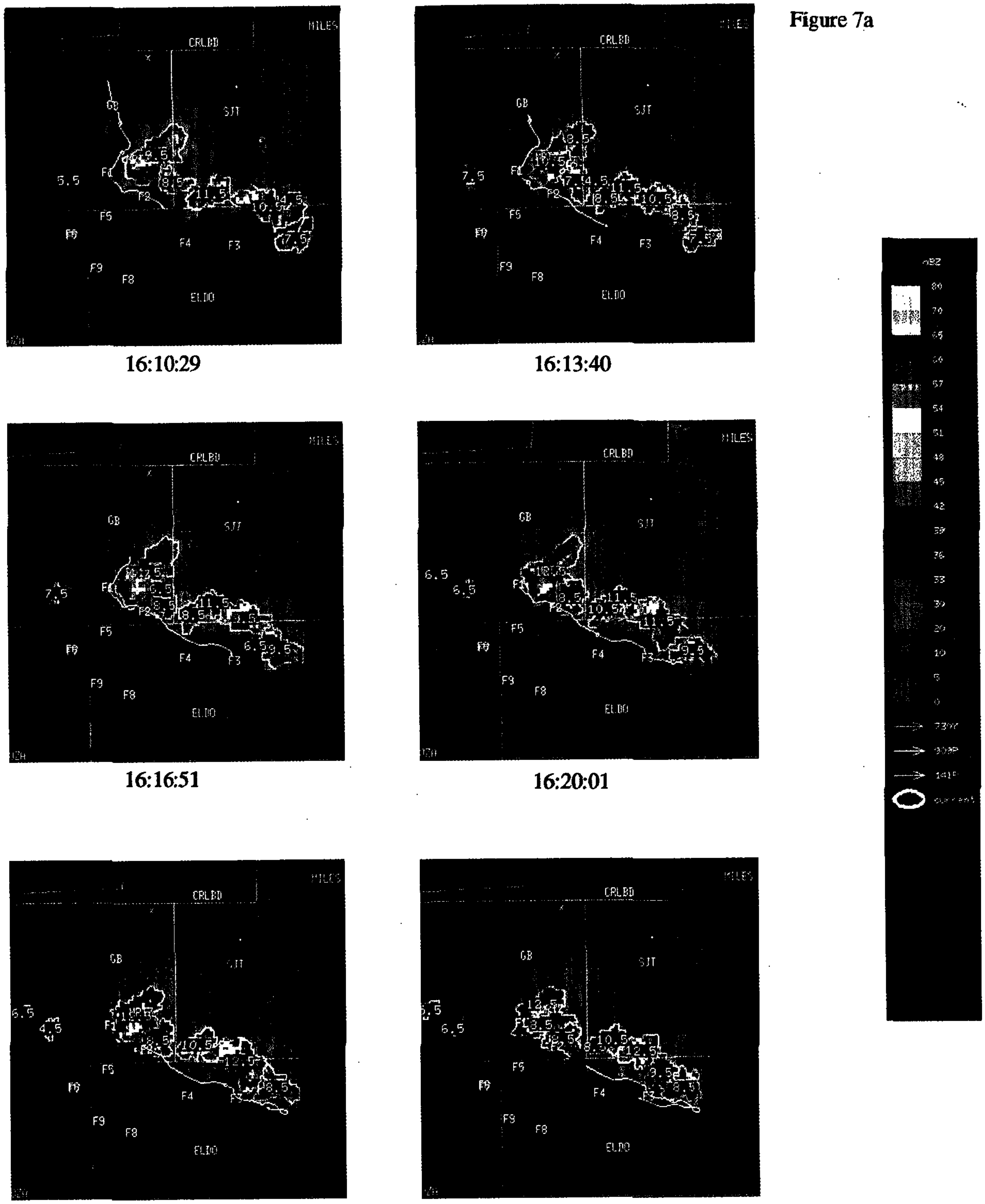

Figure 7. Documentation of the development of radar echoes in the WTWMA target from 1610 CDT through 1724 CDT on 28 August 1999 using the TITAN system. The echo tops and the color-contoured echo intensities are as shown. The latter can be quantified using the scale on the right of each presentation. The track of the seeder aircraft with time is shown by the white line. Identifiers F1-F9 indicate the locations where burn-in-place (BIP) flares were ignited. The times and locations of each BIP flare are provided in Table 1.

"REVIEWED"

August 28, 1999

Figure 7b

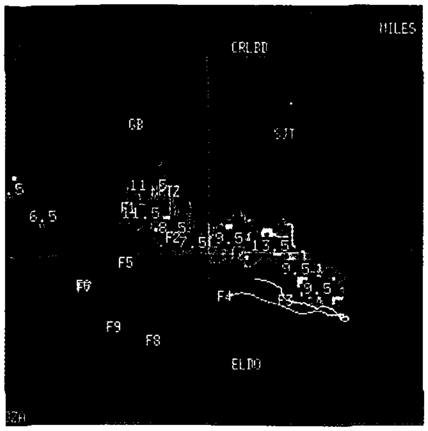

16:29:23

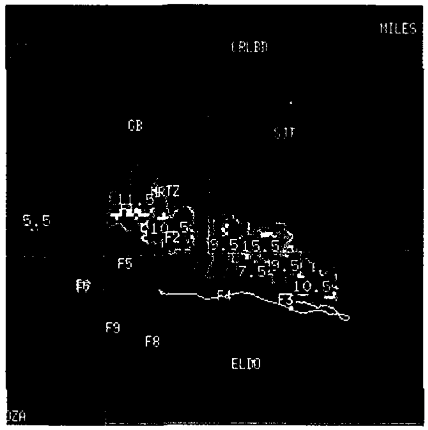

16:32:45

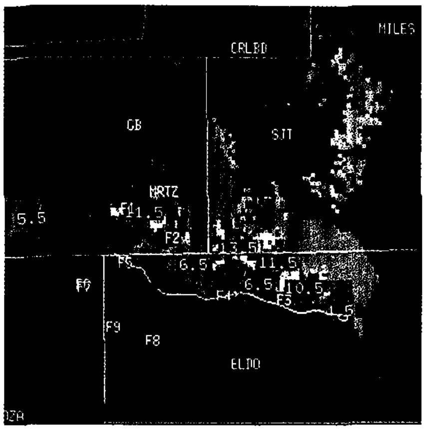

16:35:56

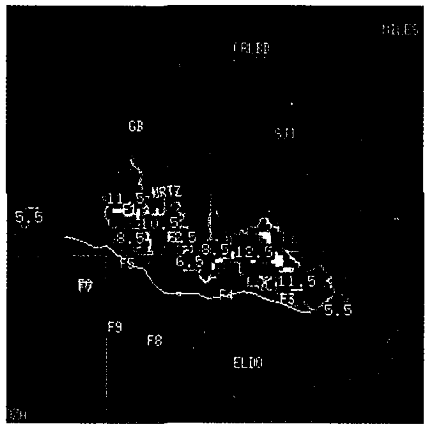

16:39:07

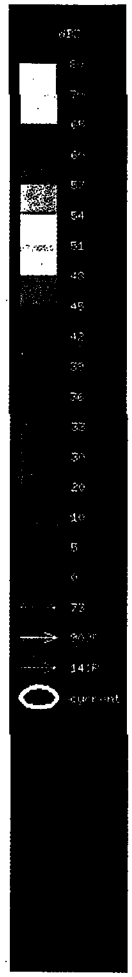

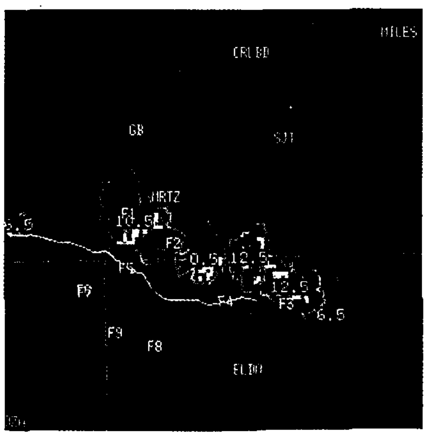

16:42:18

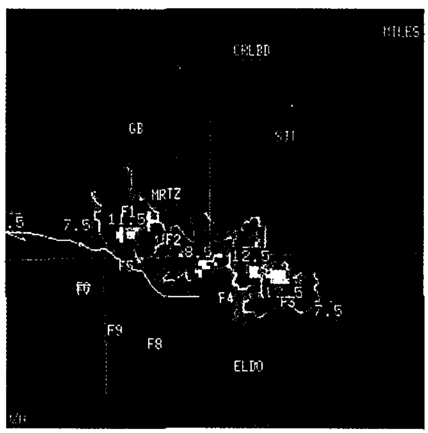

16:45:29

August 28, 1999

Figure 7c

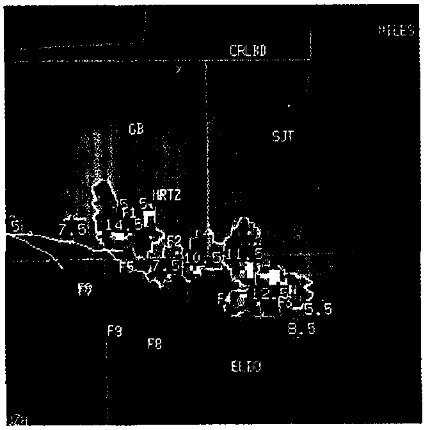

16:48:40

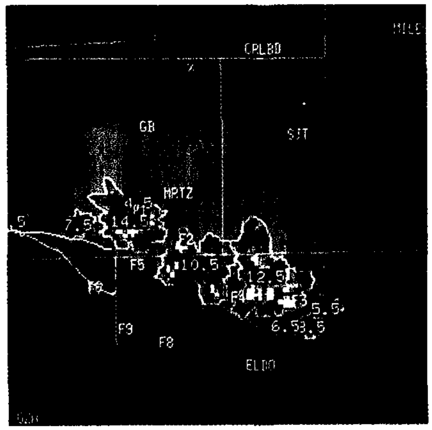

16:51:50

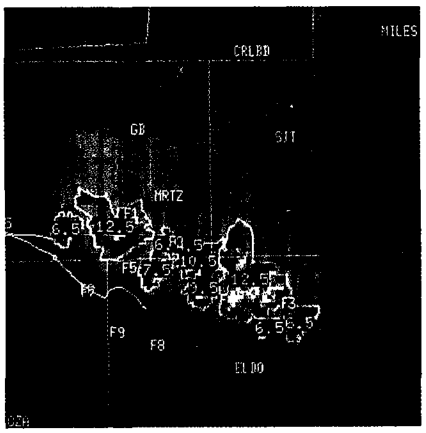

16:55:02

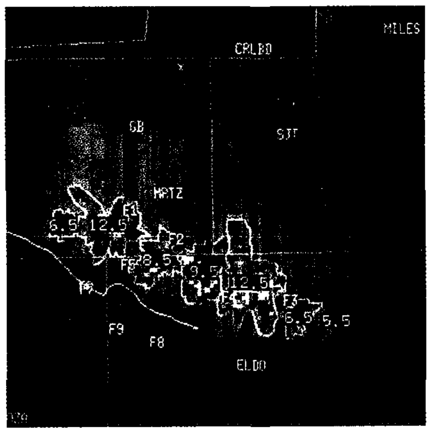

16:58:13

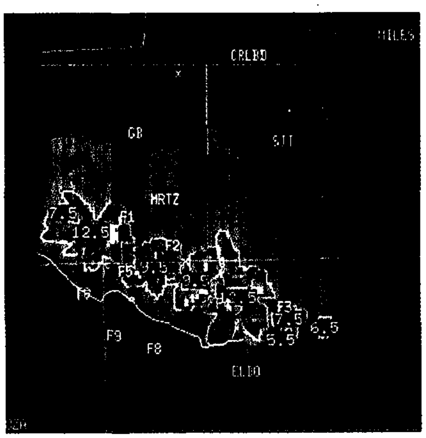

17:01:24

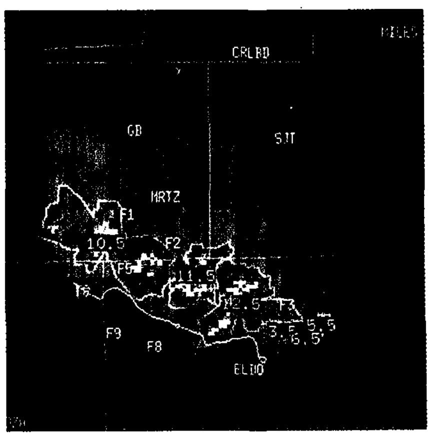

17:04:35

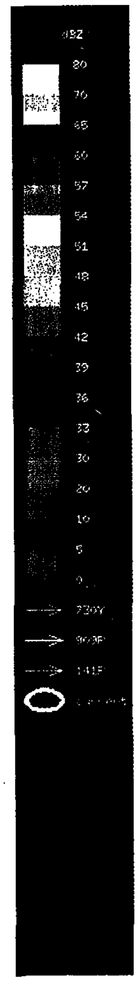

August 28, 1999

Figure 7d

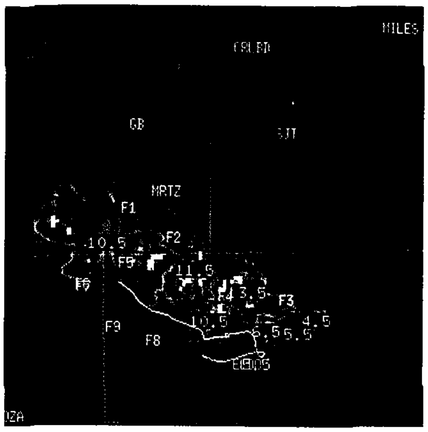

17:07:46

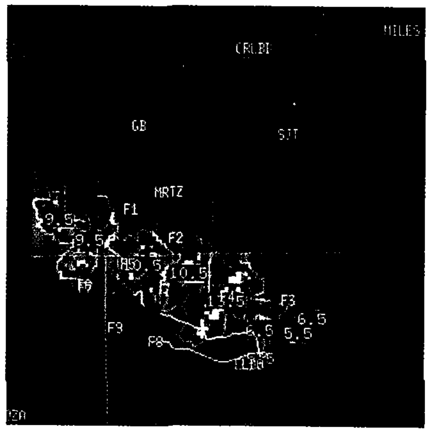

17:10:57

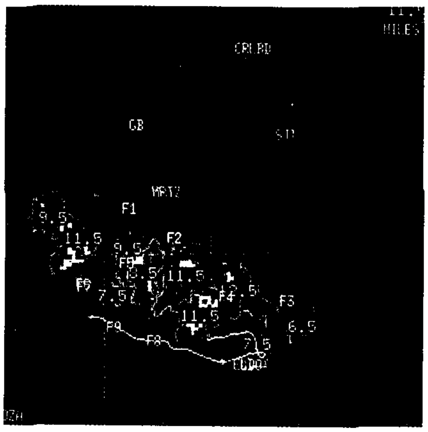

17:14:07

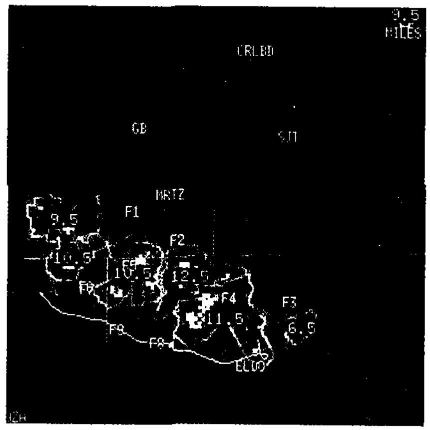

17:17:18

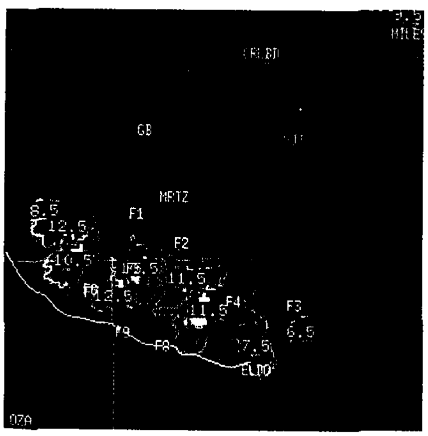

17:20:29

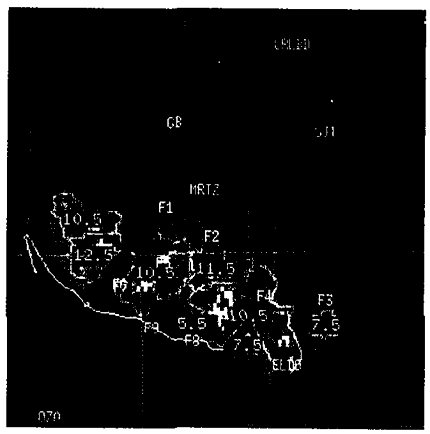

17:23:40

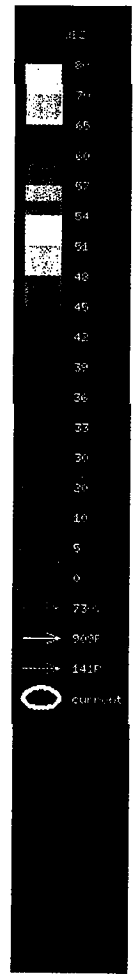

Table 1. Documentation of Seeding Activity in the WTWMA Target on 28 August 1999

Time (CDT)	Action	Comments
1615	BIP at 235/23	Cld bases at 10,600 ft, 1,000 ft/min, 32 sec BT
1619	BIP at 219/21	Updraft 1,500 ft/min in SE Irion
1627	BIP at 170/23 30.97;100.48	Updraft 1,000 ft/min in N Schleicher
1639	BIP at 189/22 30.99; 100.63	Aircraft at 10,400 ft; Est. T = 10C Updraft 2,000 ft/min
1645	BIP at 223/28 31.96; 100.91	Aircraft at 10,600 ft Updraft 1,500 ft/min
1701	2 BIP at 225/34 31.00; 101.03	At 10,200 ft, Est. T = 11C, Updraft 3,000 ft/min Satellite Overpass at 1703 CDT
1720	BIP at 205/34 30.88; 100.85	At 10,500 ft, Updraft 1,500 ft/min
1723	BIP at 212/35 30.99; 100.94	At 10,400 ft, Updraft > 1,500 ft/min
1730	BIP at 240/42 31.09; 101.25	At 10,500 ft, Updraft 1,500 ft.min
1742	BIP at 218/41 30.87; 101.07	At 10,400 ft, Updraft 1,500 to 2,000 ft/min
1751	BIP at 187/35 30.75; 100.68	At 10,300 ft in north-central Schleicher County, Est. T = 11C , Updraft 700 ft/min
1816	BIP in NW Crockett County	At 10,200 ft, Updraft 1,000 ft/min
1825	BIP in N Crockett County	At 10,200 ft, Est. T = 13C Updraft 1,000 ft/min
1908	BIP at 277/54 31.58; 101.51	At 10,800 ft in northern Reagan County, Est. T = 10C, Updraft > 1,000 ft/min
1910	BIP in N Reagan County	Updraft 1,500 ft/min
1912	BIP in NE Reagan County	At 10,400 ft, Est. T = 9C Updraft 2,000 ft/min
1919	BIP in N Irion County	

Note: One AgI generator was on continuously from 1607 CDT to 1852 CDT

Return to Figure 6 and note the plots of the effective cloud radius (r_{eff}) vs. temperature for clouds in Areas 1, 2 and 3. These plots appear as inserts on the left side of the image. No clouds in Area 3 received AgI treatment, because they were well outside the WTWMA target to the east. The plot for the clouds in area 3 shows a deep zone of diffusional droplet growth as indicated by the vertical yellow line. Above that were the mixed phase zone (the vertical magenta line) beginning at –19°C and the glaciated zone (vertical red line) beginning at -30°C. The median or 50th percentile plot for the effective radius (the interface between the yellow and green lines) reaches 15 microns (vertical white line) at –19°C in coincidence with the onset of the mixed phase zone. This is the region in which it is estimated that the clouds in Area 3 first developed particles of precipitation size.

Area 2 is to the east of the seeded cloud line. The clouds in this area also had a deep zone of diffusional droplet growth overlain by a shallow zone of coalescence growth. Mixed phase is indicated, beginning at about –10°C, but glaciation does not occur until about -20°C. According to the T-reff curve some cloud elements do not glaciate until T<-30°C.

The plot for the clouds in area 1, which includes the seeded line, is different from those for clouds in areas 2 and 3. The median plot for the effective radius (interface between yellow and green) reaches 15 microns at –7°C and complete glaciation at about –9°C (the bottom of the vertical red line). This early glaciation at –9°C appears to be a strong glaciation signature resulting from the seeding at cloud base. None of the clouds elsewhere are glaciated at such a warm temperature. Note also that the percentile plots for the clouds in area 1 show more variability than those in areas 2 and 3. This may be due to a mixture of the seeded and natural profiles.

Note the plot of r_e is quite noisy in the glaciated zone, especially around –20°C, where the estimated particle sizes drop to around 20 microns radius and then climbs back to > 30 microns. This indicates that the particles vary in size within the upper parts of the feeder clouds, suggesting that the seeding material had not reached the entire cloud volume uniformly, leaving some pockets of supercooled water. This agrees with other analyses (not shown), which indicate that the seeding signature is strongest in the western portion of the line.

4. DISCUSSION

The detection of apparent seeding signatures in Texas is an important development. It indicates that the top and base AgI seedings are producing ice at temperatures around –10°C. According to the conceptual model guiding the operational seeding programs in Texas, this should be the first step in the process leading to more rainfall. The TEXARC research program has already established that the seeding agents used in Texas produce more ice in individual clouds (Rosenfeld and Woodley, 1997), but such glaciation has never been documented on a scale that can be seen by satellite sensors until this study. There is now greater reason to take the next step and look for increases in rainfall as a result of the seeding.

The first step in the evaluation will make use of AVHRR satellite imagery and the Rosenfeld technique to infer the micophysical structure of the clouds on each day of seeding. These inferences will then be used to partition the overall data into microphysical categories. At the two extremes are clouds exhibiting deep diffusional growth, no coalescence and delayed glaciation and clouds with little to no diffusional growth, rampant coalescence and early glaciation. The evaluation for seeding effects will then be done within each microphysical category, since the effects of seeding likely will a function of cloud microphysical structure. Certainly, clouds with intense coalescence that are totally glaciated by –10°C should not be responsive to either a glaciogenic or hygroscopic seeding agent. Thus, evaluation within each microphysical category will decrease the overall natural variability and increase the chances of detecting a seeding effect. If no seeding effect is evident for the clouds identified most suitable by the conceptual model, there will be reason to question either the conceptual model or the execution of the seeding.

The Rosenfeld satellite method also makes it possible to evaluate the effects of seeding within a particular microphysical partition for all seeding targets. This will increase the sample size and increase the probability of detecting a seeding effect, given that one actually exists. This is a major positive development for the evaluation of both randomized and operational cloud seeding experiments.

A third use of the satellite technique might be to evaluate the relative effectiveness of base vs. on-top glaciogenic seeding in producing microphysical seeding signatures. The results presented here demonstrate that seeding signatures were produced by both base and on-top seeding in Texas. Whether one is better than the other in producing the signatures and presumably enhancing the rainfall is unknown. The likely answer will prove to be that the method of seeding should be adapted to the conditions and neither base nor top seeding is best for all conditions.

5. CONCLUSIONS

These case studies have resulted in the following conclusions:

- Top seeding appears to have produced a strong microphysical seeding signature on 10 August 1999.

- Base AgI seeding in a strong convective line in the WTWMA target on 28 August 1999 also produced a microphysical seeding signature that could be seen from space.

- The continuous burn of the AgI generator and supplemental seeding with burn-in-place AgI flares in regions of strong updraft was well adapted to the conditions.

- The seeding agent likely worked in the clouds on both days to produce more ice at warmer temperatures as intended.

- The method of seeding should be adapted to the conditions. No method of seeding is right for all conditions.

- Because more ice is being produced in the seeded clouds as required by the conceptual model guiding the operational seeding programs, there is more reason to look for augmentation of the rainfall as a consequence of the seeding.

- Although the results of this study are highly encouraging, additional cases with comparable results must be obtained to strengthen the conclusions reached here.

6. ACKNOWLEDGEMENTS

This study was funded by the Texas Natural Resource Conservation Commission (TNRCC) through a contract with Woodley Weather Consultants. The authors thank Mr.. George Bomar, Senior Meteorologist at the TNRCC, and Mr. Dale Bates, President of the WTWMA, for their encouragement during the course of this study.

7. REFERENCES

Bomar, G.W., W.L. Woodley and D.L. Bates, 1999: The Texas Weather Modification Program: Objectives, Approach and Progress. J. Wea. Mod., **31**, 9-22.

Lensky, M.I. and D. Rosenfeld, 1997: Estimation of precipitation area and rain intensity based on the microphysical properties retrieved from NOAA AVHRR data. J. Appl. Meteor., **36**, 234-242.

Nakajima, T., and M. D. King, 1990: Determination of the optical thickness and effective particle radius of clouds from reflected solar radiation measurements. Part I: Theory. J. Atmos. Sci., **47**, 1878-1893.

Rosenfeld, D., and W. L. Woodley, 1993: Effects of cloud seeding in west Texas: Additional results and new insights. J. Appl. Meteor., 32, 1848-1866.

Rosenfeld, D. and G. Gutman, 1994: Retrieving microphysical properties near the tops of potential rain clouds by multispectral analysis of AVHRR data. J. Atmos. Res. **34**, 259-283.

Rosenfeld, D. and W.L. Woodley, 1997: Cloud microphysical observations of relevance to the Texas cold-cloud conceptual seeding model. J. Wea. Mod., **29**, 56-69.

Rosenfeld, D. and M.I. Lensky, 1998a: Space-borne based insights into precipitation formation processes in continental and maritime convective clouds. Bull. Amer. Meteor. Soc., **79** (11).

Rosenfeld, D. and I. M. Lensky, 1998b: Space-borne insights into precipitation formation processes in continental and maritime convective clouds, Part I: Methodology. Preprints, Conference on Cloud Physics, joint with the 14th Conference on Planned and Inadvertent Weather Modification, 17-21 August 1998, Everett, Washington. AMS. P. J28-J31.

Rosenfeld D. and W. L. Woodley, 2000: Convective Clouds with Sustained Highly Supercooled Liquid Water Until –38°C. Submitted to Nature

Woodley, W.L. and D. Rosenfeld, 1999: On the use of multi-spectral satellite imagery to infer the effects of human activity on clouds and rainfall in Texas. Final Report to the Texas Natural Resource Conservation Commission from Woodley Weather Consultants.